Catal Lett (2012) 142:1190–1196
DOI 10.1007/s10562-012-0884-3

Selective Hydrodeoxygenation of Guaiacol Catalyzed by Platinum Supported on Magnesium Oxide

Tarit Nimmanwudipong · Ceren Aydin · Jing Lu · Ron C. Runnebaum · Kevin C. Brodwater · Nigel D. Browning · David E. Block · Bruce C. Gates

Received: 27 June 2012 / Accepted: 27 July 2012 / Published online: 15 August 2012

Abstract The conversion of guaiacol catalyzed by Pt/MgO in the presence of H_2 was investigated with a flow reactor at 573 K and 140 kPa. Among the dozens of reaction products identified by gas chromatography (GC) and GC/mass spectrometry, the predominant ones were phenol, catechol, and (surprisingly) cyclopentanone, with others including methane, *n*-butane, butenes, *n*-pentane, and carbon monoxide. The predominant reactions were hydrodeoxygenation (with about 70 % of the guaiacol that was converted forming products that were reduced in oxygen). In contrast, when the catalyst incorporated an acidic support, Pt/γ-Al_2O_3, other reactions became kinetically significant, exemplified by transalkylation, and the selectivity to deoxygenated products was reduced to about half the value observed with Pt/MgO at guaiacol conversions in the range of about 6–20 %. Pt/MgO underwent deactivation less rapidly than Pt/γ-Al_2O_3, consistent with a lower rate of coke formation and with observations by scanning transmission electron microscopy showing that the average platinum cluster diameter, approximately 1–2 nm in each catalyst, did not change significantly during operation. The results point to the advantages of basic supports for noble metal hydrodeoxygenation catalysts.

Keywords Hydrodeoxygenation · Platinum · MgO support · Biomass conversion · Lignin · Biofuels

1 Introduction

Lignin is an underutilized component of lignocellulosic biomass, and recent research has been directed to the discovery of efficient routes for lignin conversion to fuels and chemicals [1–3]. An attractive candidate processing strategy for fuel production involves lignin pyrolysis followed by catalytic upgrading of the resulting bio-oils to remove oxygen [2, 4–6]. Because bio-oils are complex mixtures consisting of hundreds of compounds, little is understood of the chemistry of their conversion [7]. One approach to developing fundamental understanding of this chemistry involves investigations of individual bio-oil compounds, with representative examples including phenol, anisole, guaiacol, syringol, and eugenol [8–15]. Most investigations of the reactions of these compounds have been carried out with acidic catalysts such as zeolites [16–18] or metals on acidic supports [15–17, 19]. The results show that the formation of deoxygenated products, including hydrocarbons, is accompanied by acid-catalyzed reactions such as transalkylation [16, 17] and by rapid catalyst deactivation associated with carbonaceous deposits [14].

In seeking more selective and stable catalysts for guaiacol conversion, we chose the basic MgO as the support for a metal that is a good hydrodeoxygenation (HDO) catalyst,

---

Electronic supplementary material The online version of this article (doi:10.1007/s10562-012-0884-3) contains supplementary material, which is available to authorized users.

T. Nimmanwudipong · C. Aydin · J. Lu ·
R. C. Runnebaum · K. C. Brodwater · D. E. Block ·
B. C. Gates (✉)
Department of Chemical Engineering and Materials Science,
University of California, Davis, CA 95616, USA
e-mail: bcgates@ucdavis.edu

N. D. Browning
Pacific Northwest National Laboratory, Richland,
WA 99352, USA

D. E. Block
Department of Viticulture and Enology, University of California,
Davis, CA 95616, USA

platinum. To distinguish the roles of basic and acidic supports, we also made measurements with platinum on an acidic support (Pt/γ–Al_2O_3 [20]).

2 Experimental

2.1 Chemicals

Guaiacol (2-methoxyphenol, 99.5 %) was purchased from Sigma–Aldrich and used without further purification. H_2 (99.999 %) generated from deionized water by electrolysis in a Domnick Hunter gas generator (model 40H) was used as a co-reactant in the reaction experiments and in the flame ionization detectors (FIDs) of gas chromatographs. Helium (99.995 %, Praxair) was purified by passage through Agilent Technologies traps to remove traces of hydrocarbons (BHT-4), moisture (BMT-4), and oxygen (BOT-4) prior to use as an inert carrier gas in the reaction experiments and in the gas chromatographs. N_2 (99.997 %, Praxair) was purified by passage through Agilent Technologies hydrocarbon trap (BHT-4) to remove traces of hydrocarbon prior to use as an inert carrier gas in the gas chromatographs.

2.2 Catalyst Preparation

Synthesis of the supported catalyst Pt/MgO (1 wt% Pt) was performed with standard methods for the exclusion of moisture and air. MgO powder (EM Science) was mixed with deionized water to form a paste, which was dried overnight in air at 393 K. The resultant solid was ground and treated in O_2 as the temperature was ramped linearly from room temperature to 973 K and then held for 2 h, resulting in a high degree of dehydroxylation and giving a material with a surface area of about 100 m^2/g [21]. After calcination, each sample was isolated and stored in an argon-filled glovebox (MBraun, with H_2O concentration <0.5 ppm and O_2 concentration <5 ppm) until it was used. *n*-Pentane solvent (99 %, Fisher) was dried and purified by column chromatography (Grubbs apparatus, MBraun SPS) in the presence of argon. To prepare the supported platinum catalyst, platinum(II) acetylacetonate ($Pt(acac)_2$), (98 %, Strem) and the calcined MgO powder in a Schlenk flask were slurried in dried *n*-pentane that was initially at ice temperature. The stirred slurry was warmed to room temperature, and after one day the solvent was removed by evacuation for a day, so that all the platinum remained on the MgO support. The resultant solid, containing 1 wt% Pt, was stored in the argon-filled glovebox. To form supported platinum clusters, the sample was treated in a once-through flow reactor in flowing H_2 while the temperature was ramped from 298 to 673 K over a period of 1 h and then held for 8 h with the flow of H_2 continuing. After the treatment, the sample was cooled to 298 K in flowing H_2 followed by purging with helium. The sample was then transferred to the glovebox without coming in contact with air.

Pt/γ–Al_2O_3 (1 wt% Pt) was purchased from Sigma–Aldrich.

2.3 Catalytic Reaction Experiments

The catalyst, either Pt/MgO or Pt/γ–Al_2O_3 (each mixed with particles of non-porous α-Al_2O_3 in a mass ratio of 1:10) was pretreated in the reactor with a 70/30 by volume helium/H_2 mixture flowing at 100 mL(NTP)/min prior to each reaction experiment; the catalyst in the flowing gas was heated at a rate of 5 K/min to the desired reaction temperature and held for 30 min. Reactions were carried out in a continuous down-flow, once-through tubular reactor under the following conditions, with guaiacol being vaporized at 488 K: temperature, 573 K; pressure, 140 kPa; catalyst mass, 60–1000 mg. The reactor effluent was condensed in a water-cooled condenser at temperatures in the range of 285–288 K. The liquid and gas product streams were analyzed periodically by gas chromatography and gas chromatography/mass spectrometry. The reactor system, analytical instrumentation, and methods of product analysis and data analysis are reported elsewhere [20]. Mass balance closures were typically more than 95 %.

2.4 X-ray Absorption Spectroscopy

Details of the experiments and data analysis are given in Supporting Information.

2.5 Transmission Electron Microscopy

Details of the experiments are stated in Supporting Information.

3 Results

3.1 Catalyst Characterization

The dispersion of the platinum on each support is shown by the high-angle annular dark-field (HAADF) STEM images of Fig. 1. The platinum clusters on the two supports are similar in size, consisting primarily of those in the range of approximately 1–2 nm in diameter (containing roughly 40–300 atoms each, on average), along with a few having diameters greater than 3 nm (containing more than about 1,000 atoms each) [22].

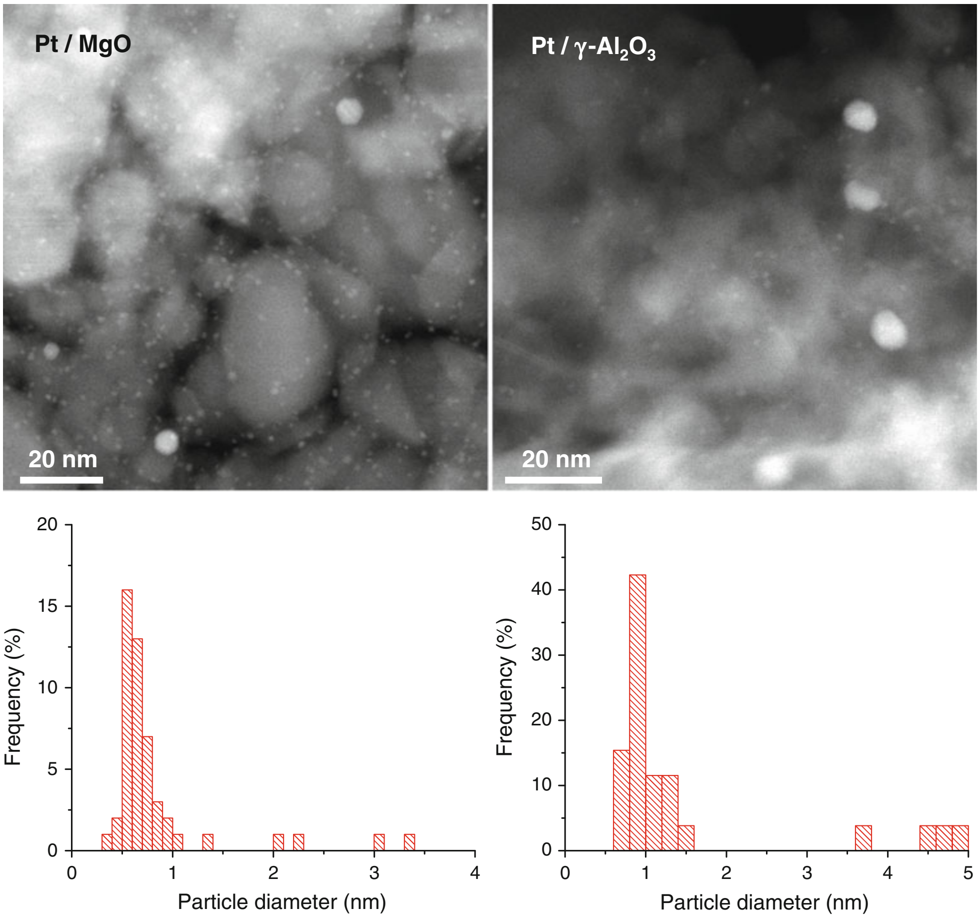

Fig. 1 HAADF–STEM images and particle size distributions of platinum supported on MgO (*left*) and on γ-Al_2O_3 (*right*)

Characterization of the catalysts by extended X-ray absorption fine structure (EXAFS) spectroscopy and X-ray absorption near edge structure (XANES) spectroscopy at the Pt L_{III} edge provided further information about the platinum species (Fig. 2). Each catalyst is characterized by a Pt–Pt contribution at a (bonding) distance of approximately 2.8 Å, and these contributions are similar in magnitude for the two catalysts and significantly different from that representing bulk platinum metal (Fig. 2). An analysis of the EXAFS data indicated first-shell Pt–Pt coordination numbers (CN) characterizing Pt/MgO and Pt/γ-Al_2O_3, respectively, of 8.1 and 8.5, together with a second-shell Pt–Pt contribution at approximately 3.9 Å with CN values of 2.5 and 2.3, respectively (Supporting Information, Table S1). The similar values for the two samples indicate similar average nuclearities of the platinum particles, corresponding to approximately 200 atoms per particle, estimated on the basis of experimental correlations [23], and consistent with the STEM results.

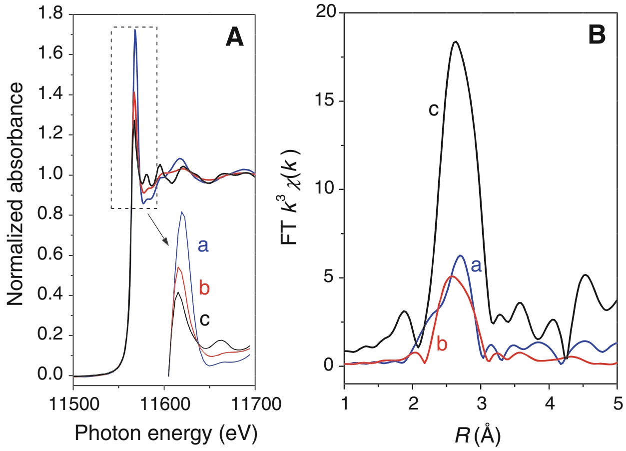

Fig. 2 XANES (**A**) and k^3-weighted magnitudes of the Fourier transforms of the EXAFS data (**B**) recorded at the Pt L_{III}-edge characterizing γ-Al_2O_3-supported platinum clusters (*a*), MgO-supported platinum clusters (*b*), and platinum foil (*c*)

XANES spectra of the two catalysts (Fig. 2) show significantly higher white line intensities than bulk platinum metal. This observation, together with the observation that the edge position of each catalyst is approximately 1.5 eV higher in energy than that of bulk platinum, indicates that the supported platinum species consist of clusters small enough

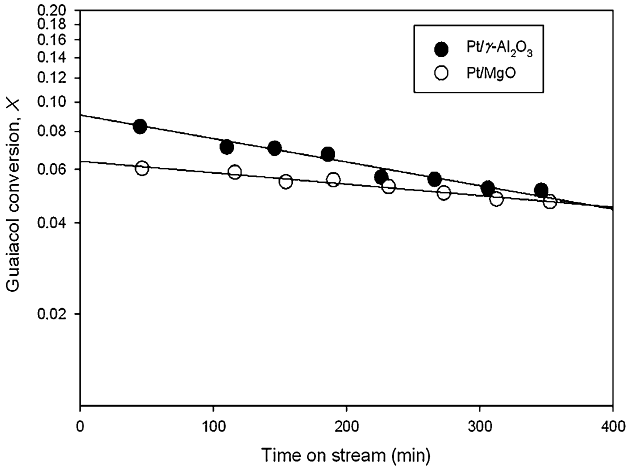

Fig. 3 Conversion of guaiacol at 573 K and 140 kPa catalyzed by Pt/γ–Al_2O_3 (*black circle*) and by Pt/MgO (*white circle*) at weight hourly space velocity (WHSV) = 11.0 (g of guaiacol)/(g of catalyst h). The feed to the flow reactor was 30 % H_2/70 % helium by volume

to have electronic properties significantly different form those of bulk platinum. Moreover, the white line intensity in the XANES spectrum characterizing Pt/γ–Al_2O_3 is greater than that characterizing Pt/MgO, indicating that the platinum in the latter has a higher electron density.

The important results of the characterization experiments are thus that the platinum species on each support consist predominantly of clusters 1–2 nm in diameter, with those on the MgO support being more electron-rich.

3.2 Catalytic Reaction Experiments

Reactions carried out in the absence of either of the catalysts in the reactor gave no evidence of the formation of products, with the exception of one, mentioned below. Activities of the catalysts were determined as the initial conversions found by extrapolating conversion data to zero time on stream (by using an exponential fit, as shown in Fig. 3). These data thus determined catalytic activities in the absence of catalyst deactivation.

Deposits accumulated on the catalysts during operation in the flow reactor. The masses of deposits (presumed to be coke) formed on the catalyst in 6 h of operation in the conversions catalyzed by Pt/MgO and by Pt/γ–Al_2O_3 were 0.004 and 0.077 g, respectively. The conversions were both approximately 0.06. The HAADF–STEM images of each catalyst before and after use showed essentially the same platinum particle size distribution.

3.2.1 Conversion of Guaiacol Catalyzed by Pt/MgO

In the guaiacol conversion catalyzed by Pt/MgO, the major products were phenol, cyclopentanone, and catechol; 93 % of the guaiacol that was converted formed one of these three products (Table 1). Other products formed with lower but still substantial selectivities included benzene, anisole, cyclohexanone, 2-methylphenol, and 1,2-dimethoxybenzene. Trace products (identified only qualitatively) included 2-pentanone, 2-pentanol, 2-cyclopenten-1-one, cyclopentanol, 2-hexanone, 3-hexanone, cyclohexanol, 2-methylcyclohexanone, 2-methylcyclohexanone, and 2-methoxycyclohexanone. Water and methanol were observed in the liquid product stream but not quantified. Several gaseous products were also observed, relatively abundant among them being methane, *n*-butane, and carbon monoxide. Traces of 1-butene, 2-butene, and *n*-pentane were also observed, but these were not quantified.

In the conversion catalyzed by Pt/MgO, the total products from which oxygen had been removed (Table 2) accounted for approximately 70 % of the guaiacol converted. (In contrast, when the catalyst was Pt/γ-Al_2O_3, the corresponding value was only approximately 30 %.)

To determine an approximate reaction network for the conversion of guaiacol catalyzed by Pt/MgO in the

Table 1 Products of conversion of guaiacol catalyzed by Pt/MgO and by Pt/γ–Al_2O_3 (liquid product streams)

Product	Selectivity[a] to product in reaction catalyzed by Pt/MgO in the presence of H_2[b]	Selectivity to product in reaction catalyzed by Pt/γ–Al_2O_3 in the presence of H_2[c]
Benzene	0.0003	0.001
Anisole	0.002	0.007
Cyclopentanone	0.17	0.006
Cyclohexanone	0.022	0.019
Phenol	0.51	0.26
o-Cresol	0.003	0.011
1,2 Dimethoxybenzene	0.008	0.024
3-Methylguaiacol	–	0.012
6-Methylguaiacol	–	0.030
Catechol	0.25	0.51
3-Methylcatechol	–	0.10

Data were extrapolated to zero time on stream, and thus represent approximate initial selectivities determined at a pressure of 140 kPa, and a temperature of 573 K

[a] Selectivity is defined as yield (mol product formed/mol of organic reactant fed)/conversion (mol of organic reactant consumed/mol of organic reactant fed)

[b] Feed rate of gas, 100 mL/min; composition, 30 % H_2/70 % helium (feed molar ratio of H_2 to guaiacol was 15). The weight hourly space velocity was 11.0 (g of reactant)/(g of catalyst h), and the approximate initial conversion was 0.064

[c] Feed rate of gas, 100 mL/min; composition, 30 % H_2/70 % helium; feed molar ratio of H_2 to guaiacol was 15. The weight hourly space velocity was 18.0 (g of reactant)/(g of catalyst h), and the approximate initial conversion was 0.066

Table 2 Major products formed in oxygen-removal reactions in the conversion of guaiacol with H_2 catalyzed by Pt/MgO

Product	Structure	Reaction class
Benzene		HDO
Anisole	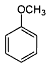	HDO
Cyclopentanone	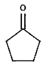	Ring opening/closing and decarbonylation[a]
Cyclohexanone	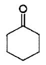	HDO and hydrogenation
Phenol	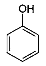	HDO
o-Cresol	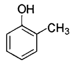	HDO and methylation[a]

[a] See text

presence of H_2, selectivity versus conversion plots (Fig. 4) were used to identify products as primary or not [24, 25]; a positive intercept indicates a primary product, whereas an intercept indistinguishable from zero indicates a higher-order product. (These designations are empirical, falling short, for example, of providing information about intermediates that were too reactive to be detected.) The selectivity–conversion data (Figs. 4, S2, S3) indicate that anisole, cyclopentanone, phenol, cyclohexanone, *o*-cresol, and catechol were all primary products, whereas benzene was a non-primary product.

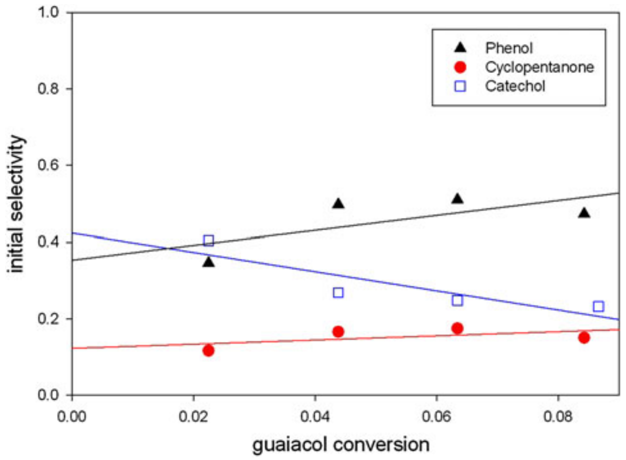

Fig. 4 Selectivity for the formation of phenol (*triangles*), cyclopentanone (*circles*), and catechol (*squares*) in the conversion of guaiacol catalyzed by Pt/MgO; reaction conditions are stated in Table 1. Data for each product were fitted with a straight line and extrapolated to zero conversion; intercepts of regression lines significantly different from zero selectivity at zero conversion (analyzed with 95 % confidence limits) indicate primary products, in this case all: phenol, cyclopentanone, and catechol

Selectivity data collected with Pt/MgO at a higher guaiacol conversion (approximately 0.2) are also summarized in Supporting Information, Table S3; the values are similar to those observed at the lower conversion (Table 1).

3.2.2 *Conversion of Guaiacol Catalyzed by Pt/γ-Al_2O_3*

The products formed in the guaiacol conversion catalyzed by Pt/γ–Al_2O_3 are listed in Supporting Information, Table S2. Additional data characterizing the performance of this catalyst are reported elsewhere [16, 27].

4 Discussion

The selectivity–conversion data (e.g., Fig. 4) and the identities of the products (Table 1) provide a basis for inferring the kinetically significant classes of reaction. These include reactions that remove oxygen from guaiacol, including hydrodeoxygenation (HDO), hydrogenolysis, and perhaps others that are mentioned below.

4.1 Reactions of Guaiacol Catalyzed by Pt/MgO

Our data show that in the conversion catalyzed by Pt/MgO, phenol and anisole were primary products, inferred to have formed by HDO, a reaction in which a C–O bond is cleaved with removal of an oxygen atom from the guaiacol. HDO of guaiacol involves breaking of a C–O bond to form water or methanol. Thus, the products of guaiacol HDO include phenol—the product formed in highest yield. The minor product anisole (along with water) is evidence of a different HDO reaction. The data also suggest the occurrence of secondary HDO reactions—of phenol and of anisole, each to form benzene. Thus, we suggest that benzene was not a primary product.

We contrast HDO with hydrogenolysis, which is a reaction in which a C–O bond is cleaved without necessarily removing an oxygen atom from the guaiacol; an example is the reaction of anisole to give methane and phenol. Thus, the observation of catechol and methane as products suggests the occurrence of hydrogenolysis of guaiacol (at the methoxy group).

The reactions leading to the formation of cyclopentanone are also kinetically important. This product was unexpected. The transformation giving this product, involving loss of a carbon atom from guaiacol, might be associated with the formation of carbon monoxide (as was observed), possibly via ring opening and decarbonylation. This suggestion implies that cyclopentanone was not a primary product, although the conversion–selectivity plot

(Fig. 4) is consistent with such a designation—even though it does not distinguish primary products from higher-order products when the latter are formed via highly reactive, undetectable intermediates. Consequently, we suggest that the non-zero selectivity for formation of cyclopentanone at zero guaiacol conversion implies high rate of cyclopentanone formation.

The route to the formation of the minor product *o*-cresol is also unobvious. A recent report [26] suggests that this compound can be formed in the reaction of phenol and methanol on MgO. Our data are consistent with this suggestion, as we observed both phenol and methanol as primary products. As a result, we suggest that *o*-cresol was also a non-primary product.

4.2 Comparison of Pt/MgO and Pt/γ–Al_2O_3 as Catalysts for Conversion of Guaiacol

The products formed in the guaiacol conversion catalyzed by Pt/γ–Al_2O_3 match those in an earlier report [16, 27] in terms of product distributions and kinetically significant reaction classes.

The high selectivity observed for phenol formation from guaiacol with each catalyst suggests the importance on each catalyst of HDO occurring at the methoxy group. Consistent with results reported for the conversion catalyzed by Pt/γ-Al_2O_3, the results point to the platinum as the catalyst for HDO.

Catechol is another major product that was observed with each of the catalysts. At similar conversions, the selectivity for catechol formation was higher in the conversion catalyzed by Pt/γ–Al_2O_3 than in that catalyzed by Pt/MgO (Table 1). In the absence of acidic sites, catechol is expected to form on Pt/MgO primarily by hydrogenolysis on the platinum, with methane as a co-product. On Pt/γ-Al_2O_3, in contrast, catechol can also form on the acidic support (along with methylguaiacol) by transalkylation (e.g., 2 guaiacol → catechol + 6-methylguaiacol), as described elsewhere [27]. Thus, we observed methylated guaiacol and methylated catechol in the conversion catalyzed by Pt/γ–Al_2O_3 but not Pt/MgO. The γ–Al_2O_3 support can catalyze both unimolecular and bimolecular transalkylation reactions to produce those methylated products.

1,2-Dimethoxybenzene and *o*-cresol, which are formed by acid-catalyzed transalkylation reactions in the conversion catalyzed by Pt/γ-Al_2O_3, were formed only minimally in the conversion catalyzed by Pt/MgO. We infer that 1,2-dimethoxybenzene was formed from guaiacol in a non-catalytic reaction, as it was observed (as the only product) in blank experiments (without catalyst), with the conversions being <0.0005.

A relatively high selectivity for cyclopentanone formation was observed with Pt/MgO but not Pt/γ-Al_2O_3. The observed formation of carbon monoxide on Pt/MgO (only traces were observed in the conversion with Pt/γ-Al_2O_3) suggests that cyclopentanone was produced from catechol in a sequence of reactions, which might involve ring hydrogenation, ring-opening and closing, and decarbonylation. Ring-opening reactions catalyzed by metals are well known [28, 29].

By recognizing which compounds were primary and which were non-primary and by using our judgment of the most likely classes of reaction for formation of the minor products, we inferred the preliminary reaction network of Fig. 5 for guaiacol conversion catalyzed by Pt/MgO in the presence of H_2. The dashed arrows represent transalkylation reactions observed in the reactions with Pt/γ–Al_2O_3 but not with Pt/MgO.

The data show that Pt/γ–Al_2O_3 gave a higher initial conversion of guaiacol than Pt/MgO, but Pt/MgO underwent deactivation less rapidly than Pt/γ–Al_2O_3 (Fig. 3). We observed deposits (black, evidently carbonaceous materials) on the used Pt/γ–Al_2O_3 catalyst but barely on the used Pt/MgO. The observations suggest that coking was a cause of deactivation of the former. Because the HAADF–STEM images of the catalysts before and after use (Fig. S1) show

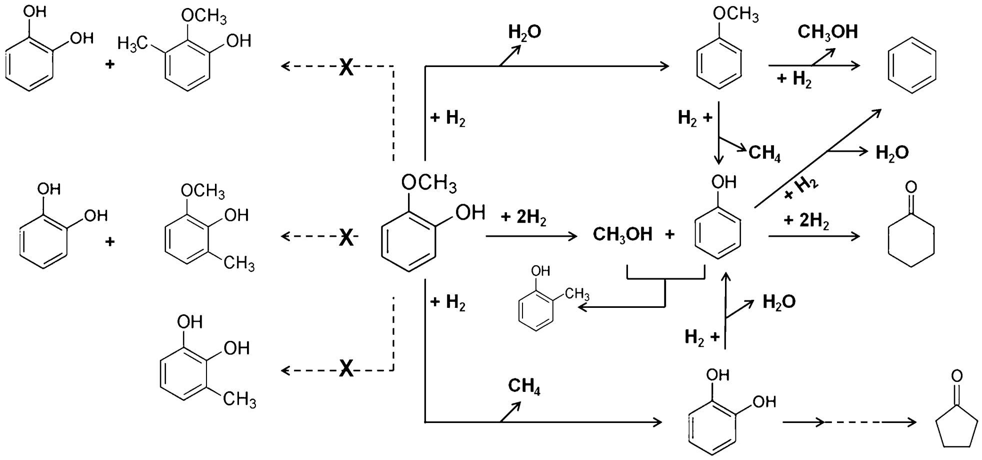

Fig. 5 Reaction network for the conversion of guaiacol and H_2 catalyzed by Pt/MgO at 573 K. Reactions are postulated on the basis of the products identified, including trace compounds, and their formation as a result of the likely reaction classes identified in the text. Hydrogenation/dehydrogenation/hydrodeoxygenation reactions are represented by *solid arrows*. Transalkylation reactions occur only on Pt/γ–Al_2O_3 and are represented by *dashed arrows*

that there were no significant changes in the platinum cluster diameters during operation at 573 K, the data weigh against sintering of the platinum as a significant cause of catalyst deactivation.

In summary, the results demonstrate that Pt/MgO is a more selective catalyst for oxygen removal from guaiacol in the presence of H_2 than Pt/γ-Al_2O_3, the acidic sites of which catalyze transalkylation reactions. Moreover, Pt/MgO is more stable than Pt/γ–Al_2O_3 because of the relative lack of coke formation.

5 Conclusions

In the conversion of guaiacol catalyzed by platinum supported on the basic metal oxide MgO, in the presence of H_2, the important reaction classes include HDO, hydrogenolysis, and hydrogenation. The conversion catalyzed by Pt/γ–Al_2O_3 is characterized by an additional reaction class, acid-catalyzed transalkylation. The selectivity to deoxygenated products in the reactions on Pt/MgO was approximately double the value achieved with Pt/γ-Al_2O_3. Pt/MgO, in contrast to Pt/γ-Al_2O_3, surprisingly catalyzed the formation of the cyclic deoxygenated product cyclopentanone at a relatively high selectivity along with C_4 hydrocarbons and carbon monoxide. The data suggest the occurrence of sequential reactions (presumably involving ring opening, ring closing, and decarbonylation) on Pt/MgO, but not on Pt/γ-Al_2O_3. Besides being more selective than Pt/γ-Al_2O_3, Pt/MgO underwent deactivation less rapidly than Pt/γ-Al_2O_3. The results point to the potential value of basic supports for metal catalysts for HDO of bio-oils.

Acknowledgments This research was funded by a fellowship provided by Chevron (T.N.), by the Ernest Gallo Endowed Chair in Viticulture and Enology, and by DOE (Basic Energy Sciences) Grant No. DE-FG02-03ER46057 (C.A.), Grant No. DE-SC0005822 (J.L.), and the University of California Lab Fee Program. We thank Kevin Tay and Leng Mut for help with the experiments. An Agilent Technologies Foundation Research Project Gift provided a GC7890 Refinery Gas Analyzer. We acknowledge beam time and the support of the DOE Division of Materials Sciences for its role in the operation and development of beam line X-18B at the National Synchrotron Light Source (NSLS) at Brookhaven National Laboratory. We thank the beamline staff for valuable support.

References

1. Zakzeski J, Bruijnincx PCA, Jongerius AL, Weckhuysen BM (2010) Chem Rev 110:3552
2. Huber GW, Iborra S, Corma A (2006) Chem Rev 106:4044
3. Calvo-Flores FG, Dobado JA (2010) Chem Sus Chem 3:1227
4. Czernik S, French R (2010) Fuel Proc Technol 91:25
5. Elliot DC (2007) Energy Fuels 21:1792
6. Pandey MP, Kim CS (2011) Chem Eng Technol 34:29
7. Choudhary TV, Phillips CB (2011) Appl Catal A 397:1
8. Gutierrez A, Kaila RK, Honkela ML, Siloor R, Krause AOI (2009) Catal Today 147:239
9. Zhao HY, Li D, Bui P, Oyama ST (2010) Appl Catal A 391:305
10. Bui VN, Laurenti D, Afanasiev P, Geantet C (2010) Appl Catal B 101:239
11. Zhao C, Kou Y, Lemonidou AA, Li X, Lercher JA (2009) Angew Chem Int Ed 48:3987
12. Runnebaum RC, Nimmanwudipong T, Limbo RL, Block DE, Gates BC (2012) Catal Lett 142:7
13. Jongerius AL, Jastrzebski R, Bruijnincx PCA, Weckhuysen BM (2012) J Catal 285:315
14. Nimmanwudipong T, Runnebaum RC, Ebeler SE, Block DE, Gates BC (2012) Catal Lett 142:151
15. Zhu X, Lobban LL, Mallinson RG, Resasco DE (2011) J Catal 281:21
16. Nimmanwudipong T, Runnebaum RC, Block DE, Gates BC (2011) Catal Lett 141:779
17. Runnebaum RC, Nimmanwudipong T, Block DE, Gates BC (2011) Catal Lett 141:817
18. Zhu X, Mallinson RG, Resasco DE (2010) Appl Catal A 379:172
19. Hong DY, Miller SJ, Agrawal PK, Jones CW (2010) Chem Commun 46:1038
20. Runnebaum RC, Lobo-Lapidus RJ, Nimmanwudipong T, Block DE, Gates BC (2011) Energy Fuels 25:4776
21. Uzun A, Ortalan V, Browning ND, Gates BC (2009) Chem Commun 31:4657
22. Lin Y, Finke RG (1994) J Am Chem Soc 116:8335
23. Jentys A (1999) Phys Chem Chem Phys 1:4059
24. Bhore NA, Klein MT, Bischoff KB (1990) Ind Eng Chem Res 29:313
25. Bhore NA, Klein MT, Bischoff KB (1990) Chem Eng Sci 45:2109
26. Cavani F, Lercher JA (2010) J Catal 269:340
27. Nimmanwudipong T, Runnebaum RC, Block DE, Gates BC (2011) Energy Fuels 25:3417
28. Maire G, Plouidy G, Prudhomme JC, Gault FG (1965) J Catal 4:556
29. McVicker GB, Daage M, Touvelle MS, Hudson CW, Klein DP, Baird WC Jr, Cook BR, Chen JG, Hantzer S, Vaughan DEW, Ellis ES, Feeley OC (2002) J Catal 210:137